

ECGadv: Generating Adversarial Electrocardiogram to Misguide Arrhythmia Classification System

Huangxun Chen^{1†}, Chenyu Huang^{1†}, Qianyi Huang¹, Qian Zhang¹, Wei Wang²

¹ The Hong Kong University of Science and Technology

² Huazhong University of Science and Technology

{hchenay, chuankak}@connect.ust.hk, qhuangaa@ust.hk, qianzh@cse.ust.hk, weiwangw@hust.edu.cn

[†] Co-primary Authors

Abstract

Deep neural networks (DNNs)-powered Electrocardiogram (ECG) diagnosis systems are recently emerging, and are expected to take over tedious examinations by cardiologists. However, their vulnerability to adversarial attacks still lack comprehensive investigation. ECG recordings differ from images in the visualization, dynamic properties and accessibility. Thus, the existing image-targeted attack may not be directly applicable. To fill this gap, this paper proposes ECGadv to explore the feasibility of adversarial attacks on the arrhythmia classification system. We identify the main issues under two different deployment models (*i.e.*, cloud-based and local-based) and propose effective attack schemes respectively. Our results demonstrate the blind spots of DNN-powered diagnosis systems under adversarial attacks, which facilitates future research on countermeasures.

1 Introduction

Statistics [World Health Organization, 2018] show that cardiovascular diseases are the leading health problem and cause of death worldwide. In common clinical practice, the ECG is an important tool to diagnose a wide spectrum of cardiac disorders. Traditionally, cardiologists review ECG recordings to identify abnormalities, which rely heavily on manual labor and medical expertise. The Deep Neural Networks (DNNs)-powered approaches [Kiranyaz *et al.*, 2016; Al Rahhal *et al.*, 2016; Awni Y *et al.*, 2019; IEEE-Spectrum, 2018] have been the main workhorse of recent advances in automatic ECG classification and diagnosis. With strong capabilities of autonomously learning features from raw data, DNNs-powered approaches have drawn a remarkable amount of public attention and enabled the low-cost, accurate and early cardiac diagnosis to be widely available. Advanced DNNs-based ECG classification models can either work in smart devices (*e.g.*, Apple Watch) to provide real-time ECG monitoring (*i.e.*, local deployment model), or be located on the cloud to facilitate tele-medicine for chronic sufferers at home or in rural communities (*i.e.*, cloud deployment model).

Despite their great potential, DNNs' broad adoption has also aroused public concern about the reliability of the algorithm on which people's health and lives rely upon. Thus, there is an urgent need to investigate any possible breaches and vulnerabilities of DNN-based diagnosis systems.

Previous discussion on DNN model attacks mainly focus on the image domain. In the image domain, the state-of-the-art literature has shown that an adversary can construct adversarial images by adding almost imperceptible perturbations to the input image. This misleads DNNs to misclassify them into an incorrect class [Szegedy *et al.*, 2013; Goodfellow *et al.*, 2014; Carlini and Wagner, 2017]. Although extensive efforts have been devoted to the image domain, the adversarial attack in the medical measurement domain has been overlooked. ECG recordings depart from traditional images along three axes. In terms of visualization, ECGs are in a time-amplitude format while images are in 2D color format. Each value in an ECG represents the voltage of a sample point which is visualized as a line curve for examination. Meanwhile, each value in a image represents the grayscale or RGB value of a pixel which is visualized as the corresponding color for demonstration. In terms of dynamic properties, medical data present more periodicity while images present more locality. In terms of accessibility, images are more accessible due to the boom of the Internet and social media, while ECGs are regarded as private data and have high acquisition costs for an adversary.

These differences motivate us to reconsider adversarial attacks in the context of DNN-based ECG classification system. For cloud-based systems, the ECG recording may often be queried by cardiologists or patients themselves. Thus, we wonder whether it is possible for an adversary to corrupt an ECG example with sufficiently subtle perturbations and without arousing suspicion. Most image-targeted attacks utilized L_p norm to encourage visual imperceptibility of perturbations. They may not be directly applicable on an ECG because humans have different perceptual sensitivities to colors and line curves. As shown in Fig. 1, when two data arrays are visualized as line curves, their differences are more prominent rather than those visualized as gray-scale images. Thus, this paper explores proper metrics to quantify perceptual similarities of line curves, and leverages them to generate unsuspecting adversarial instances for cloud-based ECG system attacks. For the local-based systems, an adversary can corrupt an ECG via an EMI signal injection [Kune *et al.*, 2013]. However, it is hard to obtain the current sampling point of the on-the-fly ECG recordings. The mismatch may make the perturbation added to the signal at a random time stamp. In addition, it is almost impossible to obtain every ECG recording especially when they are stored locally. Thus, this paper explicitly considers a possible mismatch in an attack scheme to generate perturbations that are effective for the on-the-fly signals, and the perturbations obtained based on some instances can be applicable on other unseen ones as well.

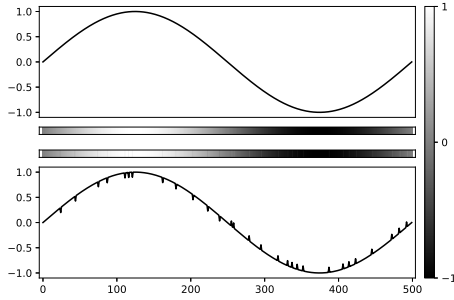


Figure 1: Perception test. There are two data arrays in the range of $[-1, 1]$, and the second one is obtained by adding a few perturbations with 0.1 amplitude to the first one. Both of them are visualized as line curves and gray-scale images.

In summary, the contributions of this paper are as follows:

- This paper takes the first step to investigate adversarial attacks in DNN-based ECG classification systems. We identify the main issues under two different deployment models (*i.e.*, cloud-based and local-based) and propose effective attack schemes respectively.
- For attacks against the cloud deployment model, this paper propose a smoothness metric to quantify human perceptual distance on line cures, which captures the pattern similarity in a computationally-efficient way (Section 4.1). Adversarial attacks using the smoothness metric achieve a 99.9% success attack rate. In addition, we conduct an extensive human perceptual study on both ordinary people and cardiologists to evaluate the imperceptibility of adversarial ECG instances (Section 5.1).
- For attacks against the local deployment model, we model the sampling point uncertainty of the on-the-fly signals within the adversarial generation scheme (Section 4.2). The generated perturbations are shift-resistant to tamper with on-the-fly signals (99.55% success rate), and generalize well in unseen examples (Section 5.2).

2 Background

In this section, we first introduce the targeted DNN-based ECG classification system for attack scheme evaluation, then we illustrate its threat models.

2.1 Targeted DNN model

We apply our attack strategies to the DNN-based arrhythmia classification system [Rajpurkar *et al.*, 2017; Andreotti *et al.*, 2017; Awni Y *et al.*, 2019]. An arrhythmia is defined as any rhythm other than a normal rhythm. Early and accurate detection of arrhythmia types is important for detecting heart diseases and choosing appropriate treatment for a patient. If the detection algorithm is mislead to classify an arrhythmia as a normal rhythm, the patient may miss the optimal treatment period. Conversely if a normal rhythm is misclassified as an arrhythmia, the patient may accept unnecessary consultation and treatment, which would result in a waste of medical resources. Thus, this paper aims to explore the blind spots of such a system and call attention to adequate countermeasures against adversarial attacks.

The original model [Rajpurkar *et al.*, 2017] adopts 34-layer Residual Networks (ResNet) [He *et al.*, 2016] to classify a 30s single-lead ECG segment into 14 different classes. However, their dataset and trained model are not public.

In the Physionet/Computing in the Cardiology Challenge 2017 [Clifford *et al.*, 2017], [Andreotti *et al.*, 2017] reproduced the ResNet approach by [Rajpurkar *et al.*, 2017] on the dataset (denoted as PhyDB) and achieved a good performance. Both their algorithm and model are available in open-source¹. The model architecture is shown in Figure 2. PhyDB dataset consists of 8,528 short single-lead ECG segments labeled as 4 classes: normal rhythm(N), atrial fibrillation(A), other rhythm(O) and noise(\surd). Both atrial fibrillation and other rhythm indicates arrhythmia. Atrial fibrillation is the most prevalent cardiac arrhythmia and can occur in sustained or intermittent episodes. ‘‘Other rhythm’’ in the dataset refers to other abnormal arrhythmia except atrial fibrillation.

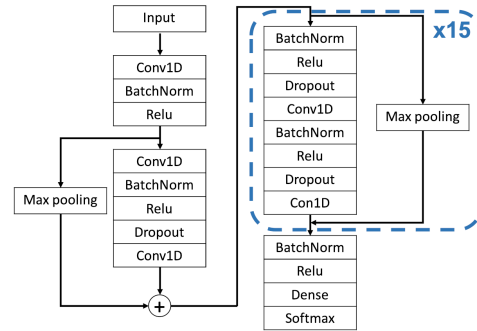


Figure 2: Architecture of Targeted Model.

2.2 Threat Models

As introduced above, DNN-based arrhythmia classification systems can be deployed on the cloud or local devices.

In the cloud deployment model, echocardiograms (ECGs) are measured using portable ECG patches like Life Signal LP1100² or household medical instruments like Heal Force ECG monitor³. Th ECGs are uploaded to the cloud through a paired smartphone/PC. The ECG classification system on the cloud conducts analysis and handles data queries from both patients and cardiologists. The attacker may conduct middle-man attacks to corrupt the data before being uploaded to the cloud. The corrupted data misleads the ECG classification system to give an incorrect diagnosis, and in the meanwhile, the data perturbations should be sufficiently subtle that they are either imperceptible to humans, or if perceptible, seems natural and not representative of an attack.

In the local deployment model, ECGs are measured and analyzed in a local device. A DNN-based ECG classification model is compressed and stored in the local device. The attacker may inject the perturbations to the on-the-fly ECG signals in real time via EMI signal injection [Kune *et al.*, 2013] to mislead the classifier. The attacker tries to maximize the success probability of attacks to disturb the normal operation of ECG monitoring devices.

3 Related Works

Here we review recent works on adversarial examples, and the existing arrhythmia classification systems.

¹<https://github.com/fernandoandreotti/cinc-challenge2>

²<https://lifesignals.com/products-services/>

³<http://www.healforce.com/en/index.php?ac=article&at=>

3.1 Adversarial Examples

In the state-of-the-art literature, considerable attack strategies have been proposed to generate adversarial examples.

Attacks can be classified into targeted and untargeted attacks based on the adversarial goal. In a targeted attack, the adversary modifies an input to mislead the targeted model to classify the perturbed input into a chosen class, while the adversary of an untargeted attack aims to make the perturbed input misclassified to any class other than the ground truth. In this paper, we only focus on the more powerful targeted attacks. According to the accessibility to the target model, the existing attacks fall into two categories, white-box and black-box attacks. In a white-box manner, an adversary has complete access to a classifier [Szegedy *et al.*, 2013; Goodfellow *et al.*, 2014; Moosavi-Dezfooli *et al.*, 2016; Carlini and Wagner, 2017; Kurakin *et al.*, 2018], while in black-box manner, an adversary has zero knowledge about them [Papernot *et al.*, 2016; Moosavi-Dezfooli *et al.*, 2017; Liu *et al.*, 2016]. In this paper, we study the adversarial attacks in the white-box setting. On one side, we would like to explore the upper bound of an adversary to better motivate defense methods. On the other side, prior works [Papernot *et al.*, 2016; Liu *et al.*, 2016] have shown the transferability of adversarial attacks, i.e., it is possible to train a substitute model given black-box access to a target model, and transfer the attacks to it by attacking the substitute one.

In the image domain, most existing works adopted L_p norm as approximations of human perceptual distance to constrain the distortion. However, for medical data in time-series format, people focus more on the overall pattern/shape, which requires other distance metrics to quantify (see Section 4.1 for more details). Recent works [Kurakin *et al.*, 2018; Athalye *et al.*, 2018b; Chen *et al.*, 2018] have explored the robustness of the adversarial examples in the physical world, where the input images could not be precisely controlled, and may change under different viewpoints, lighting and camera noise. Our attack strategy on the local deployment model is inspired by [Athalye *et al.*, 2018b; Brown *et al.*, 2017]. Different from images, we deal with sampling point uncertainty of the on-the-fly signals. For the emerging defense methods, [Athalye *et al.*, 2018a] proposed a general framework to circumvent several published defenses based on randomly transforming the input. Thus, we do not discuss defense breaking in this paper.

3.2 Arrhythmia Classification System

Considerable efforts have been made on automated arrhythmia classification systems to take over tedious examinations by cardiologists. The major challenges are the lack of feature standardization, intra-features variability and inter-patients variability [Jambukia *et al.*, 2015]. Deep learning methods show great potential due to their ability to automatically learn features through multiple levels of abstraction, which frees the system from the dependence on hand-engineered features. Recent works [Kiranyaz *et al.*, 2016; Al Rahhal *et al.*, 2016; Awni Y *et al.*, 2019] started applying DNN models on ECG signals for arrhythmia classification and achieved good performance. For any system in the health-care field, it is crucial to defend against any possible attacks since people’s lives rely heavily on the system’s reliability. Prior work [Kune *et al.*, 2013] has launched attacks to pollute the measurement of cardiac devices by a low-power emission of chosen electromagnetic waveforms. The adversarial attacks studied in this paper and the injection attacks

in [Kune *et al.*, 2013] complement each other. The injection attack can inject the carefully-crafted perturbation generated by adversarial attacks to perform targeted attacks to mislead the arrhythmia classification system on cardiac devices.

4 Technical Approach

In this section, we illustrate our attack strategies for the cloud and local deployment models respectively.

4.1 Attack Strategy for Cloud Deployment Model

Problem Formulation

Given an m -class classifier, $g : \mathcal{X} \rightarrow \mathcal{Y}$ that accepts an input $x \in \mathcal{X}$ and produces an output $y \in \mathcal{Y}$. The output vector y , treated as the probability distribution, satisfies $0 \leq y_i \leq 1$ and $\sum_{i=1}^m y_i = 1$. The classifier assigns the label $C(x) = \operatorname{argmax}_i g(x)_i$ to the input x . Let $C^*(x)$ be the correct label of x . Given a valid input x and a target class $t \neq C^*(x)$, an adversary aims to generate adversarial examples x_{adv} so that the classifier predicts $g(x_{adv}) = t$ (i.e. successful attack), and x_{adv} and x are close based on the similarity metric (i.e. visual imperceptibility). It can be modeled as a constrained minimization problem as seen in prior works [Szegedy *et al.*, 2013]:

$$\begin{aligned} & \text{minimize } \mathcal{D}(x, x_{adv}) \\ & \text{such that } C(x_{adv}) = t \end{aligned} \quad (1)$$

where \mathcal{D} is some similarity metric. It is worth mentioning that there is no box constraints for time-series measurement. It is equivalent to solve [Carlini and Wagner, 2017]:

$$\text{minimize } \mathcal{D}(x, x_{adv}) + c \cdot f_g(x_{adv}) \quad (2)$$

where f_g is an objective function mapping the input to a positive number, which satisfies $f_g(x_{adv}) \leq 0$ if and only if $C(x_{adv}) = t$. One common objective function is cross-entropy. We adopt the one in [Carlini and Wagner, 2017].

$$f_g(x_{adv}) = (\max_{i \neq t} (Z(x_{adv})_i) - Z(x_{adv})_t)^+ \quad (3)$$

where $Z(x) = z$ is logits, i.e., the output of all layers except the softmax. $(e)^+$ is short-hand for $\max(e, 0)$.

Similarity Metrics

To generate adversarial examples, we require a distance metric to quantify perceptual similarity to encourage visual imperceptibility. The widely-adopted distance metrics in the literature are L_p norms $\|x_{adv} - x\|_p$, where the p -norm $\|\cdot\|_p$ is defined as

$$\|v\|_p = \left(\sum_{i=1}^n |v_i|^p \right)^{\frac{1}{p}} \quad (4)$$

L_p norms focus on the change in each pixel value. However, human perception on line curves focuses mainly on the overall pattern/shape. Studies in [Eichmann and Zraggen, 2015; Gogolou *et al.*, 2018] show that given a group of line curves for similarity assessment, pattern-focused distance metrics like the Dynamic time warping (DTW)-based one produce rankings that are closer to the human-annotated rankings than other metrics like Euclidean distance. DTW is widely-adopted to quantify the similarity of the time series. However, the non-differentiability and non-parallelism make it ill-suited for adversarial attacks. Recent work [Cuturi and Blondel, 2017] proposes a differentiable DTW variant, Soft-DTW. However, Soft-DTW does not change the essence of DTW – a standard

dynamic programming problem. The value and gradient of Soft-DTW would be computed in quadratic time, and it is hard to leverage the parallel computing of the GPU to speed it up.

To capture the pattern similarity in a computation-efficient way, we adopt the following metric, denoted as *smoothness* as our similarity metric. Given $\delta = x_{adv} - x$ and $var(\cdot)$ refers to variance calculation:

$$\begin{aligned} diff(\delta) &= \delta_i - \delta_{i-1}, i = 2, \dots, n \\ d_{smooth}(\delta) &= var(diff(\delta)) \end{aligned} \quad (5)$$

Smoothness metric d_{smooth} quantifies the smoothness of perturbation(δ) by measuring the variation of the difference between neighbouring points of perturbation. The smaller the variation, the smoother the perturbation. A smoother perturbation δ means that the adversarial instances x' are more likely to preserve a similar pattern to the original instance x . In the extreme case where $d_{smooth} = 0$, δ should be a constant and $x_{adv} = x + \text{constant}$, i.e., the adversarial instances x_{adv} have the same pattern as the original instance x . It is worth mentioning that in our attack scheme, we intentionally preserve the zero-mean and one-variance property of the generated x_{adv} , therefore the perturbation can nor easily be filtered by the normalization layer of the system. Besides, the smoothness metric can be computed with linear time and accelerated by parallel computing as L_2 norm, which is favorable in adversarial attacks.

4.2 Attack Strategy for Local Deployment Model

Problem Formulation

Given the same m-class classifier, $g : \mathcal{X} \rightarrow \mathcal{Y}$ as in the cloud deployment model, there exists uncertainty of current sample points of the on-the-fly signal in the local deployment model. Inspired by *Expectation Over Transformation(EOT)* [Athalye *et al.*, 2018b], we regard such uncertainty as a shifting transformation of the original measurement and explicitly consider such a transformation within the optimization procedure. Given a distance function $\mathcal{D}(\cdot, \cdot)$ and a chosen distribution T of transformation function t , we aim to constrain the expected effective distance between the adversarial and original inputs:

$$\gamma = \mathbb{E}_{t \in T}[\mathcal{D}(t(x_{adv}), t(x))] \quad (6)$$

Thus, the adversarial attacks can be modeled as follows:

$$\operatorname{argmax}_{x_{adv}} \mathbb{E}_{t \in T}[\log Z(t(x_{adv}))_t] \quad (7)$$

Here we add a constraint $\mathcal{D}(t(x_{adv}), t(x)) < \epsilon$, which forces the adversarial examples to be within a certain distance constraint of the original. However, ϵ is large enough that x_{adv} can have a large probability of successful attacks under most shifting transformations. Moreover, since the ECG signals of the same class from different people are quite similar to each other, a sufficiently large ϵ can implicitly enable the universality of an adversarial sample, i.e., a perturbation can have an effect on other unseen samples of the same class.

Perturbation Window Size

Since we attack on-the-fly signals on local devices, it is better that the perturbation attracts minimal attention of the victim. Thus, we introduce a new parameter, the length of the perturbation w_d , which could be set by the adversary and fixed during the perturbation generation. w_d gives the system flexibility to control the added perturbation. The intuition behind is that the smaller w_d is, the less chance that the victim will

perceive the attack. Moreover, the larger w_d is, the generated perturbation has higher probability of having an effect on other unseen samples of the same class(i.e., universality).

5 Experimental Results

In this section, we evaluate our attacks for the cloud deployment and local deployment models respectively⁴.

5.1 Evaluation for cloud deployment model

Experiment Setup

We implement our attack strategy for the cloud deployment model under the framework of CleverHans [Papernot *et al.*, 2018]. We adopt the Adam optimizer [Kingma and Ba, 2014] with 0.005 learning rate to search for adversarial examples. We compare the performance of three similarity metrics on adversarial examples generation, given $\delta = x_{adv} - x$

- $d_{l2}(\delta) = \|\delta\|_2^2$
- $d_{smooth}(\delta)$ (Equation 5)
- $d_{smooth,l2}(\delta) = d_{smooth}(\delta) + k \cdot d_{l2}(\delta)$, $k = 0.01$

All metrics are evaluated under the same optimization scheme with the same hyper-parameters. Notice that the target model is not accurate on all ECG segments in the PhyDB dataset. Therefore, we only generate adversarial examples for those segments correctly classified by the model. The profile of the attack dataset is shown in Table 1. Here, ‘‘A, N, O, \surd ’’ denote normal rhythm, atrial fibrillation(AF), other rhythm and noisy signal respectively in the following evaluation. The sampling rate of the ECG segment is 300Hz, i.e., the length of a 30s ECG segment is 9000. The input vector of the target model in Figure 2 is 9000.

Table 1: Data profile for the attack dataset

Type	Number	Time length (s)	
		mean	std
Normal rhythm(N)	3886	32.85	9.70
Atrial Fibrillation(A)	447	32.25	11.98
Other rhythm(O)	1488	35.46	11.56
Noisy signal(\surd)	260	24.02	10.42

Success Rate of Targeted Attacks

We select the first 360 segments of class N, class A and class O respectively, and the first 220 segments of class \surd in attack dataset to evaluate the success rate of the targeted attacks. For each ECG segment, we conduct three targeted attacks to other classes one by one. Thus, we have 12 source-target pairs given 4 classes. The attack results are shown in Table 2.

With all three similarity metrics, the generated adversarial instances achieve quite high attack success rates. d_{l2} fails in a few instances of some source-target pairs, such as ‘‘O \rightarrow A’’, ‘‘A \rightarrow N’’, ‘‘O \rightarrow N’’ and ‘‘ $\surd \rightarrow$ N’’. d_{smooth} case achieves almost a 100% success rate and $d_{smooth,l2}$ achieves a 100% success rate. A sample of generated adversarial ECG signals are shown in Fig. 3. Due to the limited space, we only show a case where an original atrial fibrillation ECG(A) is misclassified to a normal rhythm(N). It is noticed that the one generated with d_{l2} metric looks more suspicious due to lots

⁴<https://github.com/codespace123/ECGadv>

Table 2: Success rates of targeted attacks (cloud-based model)

	d_{l2}				d_{smooth}				$d_{smooth,l2}$			
	A	N	O	\sim	A	N	O	\sim	A	N	O	\sim
A	/	97.22%	100%	100%	/	100%	100%	100%	/	100.0%	100.0%	100.0%
N	100%	/	100%	100%	100%	/	100%	100%	100%	/	100%	100%
O	99.44%	95.0%	/	100%	99.72%	100%	/	100%	100%	100%	/	100%
\sim	100%	99.55%	100%	/	100%	100%	100%	/	100%	100%	100%	/

of small spikes, while the d_{smooth} one preserves more similar pattern to the original. The property of $d_{smooth,l2}$ falls in between the above two as expected.

Human Perceptual Study

We conduct an extensive human perceptual study on both ordinary people and cardiologists to evaluate the imperceptibility of adversarial ECG instances. Ordinary human participants are recruited from Amazon Mechanical Turk (AMT), who do not have relevant medical expertise. Thus, they are only required to compare the adversarial examples generated using different similarity metrics and choose the one closer to the original ECG. For each similarity metric, we generate 600 adversarial examples from the PhyDB dataset (each source-target pair accounts for 50 examples). In the study, the participants are asked to observe an original example and its two adversarial ones generated using two different similarity metrics. Then they need to choose one of the two adversarial examples that is closer to the original. The perceptual study comprises three parts, (i) d_{smooth} versus d_{l2} , (ii) $d_{smooth,l2}$ versus d_{l2} , and (iii) d_{smooth} versus $d_{smooth,l2}$. To avoid labeling bias, we allow each user to conduct at most 60 trials for each part. For each tuple of an original example and its two adversarial examples, we collect 5 annotations from different participants. In total, we collected 9000 annotations from 57 AMT users. The study results are shown in Table 3, where "triumphs" denotes the metric got 4 or 5 votes for all 5 annotations, and "wins" denotes that the metric got 3 votes for 5, *i.e.*, a narrow victory.

Table 3: Human perceptual study (AMT participants)

i	d_{smooth} wins(%)			d_{l2} wins(%)		
	triumphs	wins	total	triumphs	wins	total
	58.67	22.67	81.34	10	8.66	18.66
ii	$d_{smooth,l2}$ wins(%)			d_{l2} wins(%)		
	triumphs	wins	total	triumphs	wins	total
	65.5	18.5	84	7.83	8.17	16
iii	d_{smooth} wins(%)			$d_{smooth,l2}$ wins(%)		
	triumphs	wins	total	triumphs	wins	total
	31.83	27.83	59.67	15.83	24.5	40.33

Compared with the d_{l2} -generated examples, the d_{smooth} -generated ones are voted closer to the original in 81.34% of the trials. When comparing d_{l2} and $d_{smooth,l2}$, the latter is voted as the winner in 84% of the trials. This indicates that the smoothness metric encourages generated adversarial examples preserve similar patterns to original ones, so they are more likely to be imperceptible. When comparing d_{smooth} and $d_{smooth,l2}$, d_{smooth} get a few more votes (59.67%) than $d_{smooth,l2}$, which further validates that the smoothness metric better qualifies human similarity perception on line curves than L_2 norm.

Besides participants on AMT, we also invite three cardiologists to evaluate whether added perturbations arouse their suspicion and influence their medical judgement. The cardiologists are asked to classify the given ECG and its adversarial counterparts into 4 classes (A, N, O, \sim) based on their medical expertise. As illustrated in Section 2.1, it is important to distinguish between normal and abnormal rhythms. Thus, we focus on the cases of "N \rightarrow A", "N \rightarrow O", "A \rightarrow N", "O \rightarrow N", which misclassify a normal rhythm to an arrhythmia or vice versa. For the above 4 source-target pairs, we randomly select 6 type N, 3 type A and 3 type O, then we conduct corresponding targeted attacks with different similarity metrics to generate adversarial examples. Thus, we have 48 samples (original and adversarial ones) and shuffle them randomly. For every sample, we collect annotations from all three cardiologists. The results are shown in Table 4.

Table 4: Human Perceptual Study (Cardiologists)

Idx	Original	d_{l2}	d_{smooth}	$d_{smooth,l2}$
1	100%	100%	100%	100%
2	91.7%	100%	100%	100%
3	100%	100%	100%	100%

Each row refers to one cardiologist. The first column denotes the percentage of the cardiologist's annotations which are the same as the labels in the original PhyDB dataset. Only one cardiologist annotates a type A instance as type O. The last three columns show the percentage of adversarial examples which are annotated the same type as their original counterparts. High percentage means that added perturbations do not arouse their suspicion and influence their medical judgement. The results show that in all cases, cardiologists give the same annotations to adversarial examples as their original counterparts. The possible reason is that most perturbations generally occur on the wave valley, but the cardiologists give annotations based on the peak-to-peak intervals. They think the subtle perturbations possibly caused by instrument noise.

5.2 Evaluation for local deployment model

Success Rate of Targeted Attacks

We implement our attack strategy for the local deployment model under the framework of CleverHans [Papernot *et al.*, 2018]. We maximize the objective function using the Adam [Kingma and Ba, 2014] optimizer, and approximate the gradient of the expected value through independently sampling transformations at each gradient decent step. Among 12 source-target pairs, we randomly choose 10 samples of each pair to generate adversarial perturbations by applying the attack strategy in Section 4.2. It is worth mentioning that we generate one perturbation from one sample. Thus, we have 10 perturbations from 10 samples. Then we apply the above perturbations to 100 randomly-chosen samples of the corresponding source class

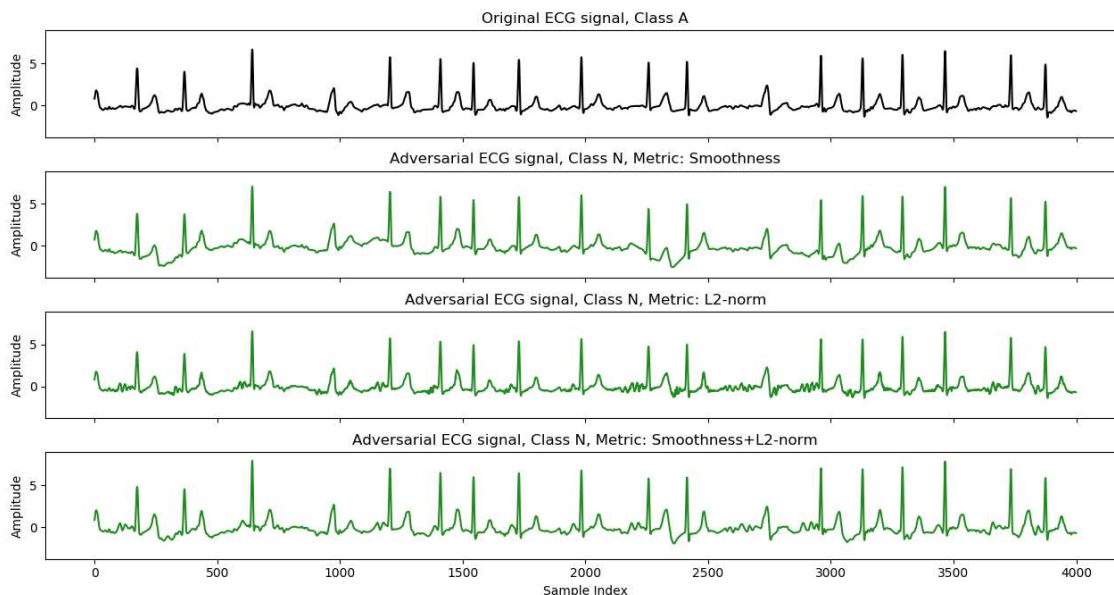


Figure 3: A sample of generated adversarial ECG signal.

to see whether the adversarial examples could mislead the classifier universally. To mimic the sample point uncertainty of the on-the-fly signals, we generate the perturbation at full length which means w_d is equal to 9000. Then we randomly shift perturbations and add them to the original signals. In this evaluation, we randomly shift the perturbations 200 times for testing. The average success rates are shown in Table 5. Our attack strategy achieves pretty high success rates, which indicates that the generated perturbation is both shift-resistant and universal.

Table 5: Success rates of targeted attacks (local model)

	A	N	O	\sim
A	/	99.87%	99.96%	99.97%
N	100%	/	100%	99.97%
O	100%	99.46%	/	100%
\sim	98.66%	98.23%	98.48%	/

Impact of Window Size

In this section, we evaluate the accuracy with different sized windows w_d .

As mentioned before, the smaller the window size, the lower the chance that the attacker can be perceived. In this evaluation, we generate perturbations on different sized windows 9000, 6000, 4500, 3000 and 1500. For each window size, we generate adversarial examples under the same conditions as the previous section – randomly 10 samples for 12 source-target pairs. Then we shift the perturbation randomly and add it to other samples from the original source class. The results are shown in Figure 4. We can see that in most cases the success rate decreases a lot when the window size increases. However, they slowly decrease and even remain almost unchanged under the cases of “A \rightarrow O”, “N \rightarrow O” and “ \sim \rightarrow O”. All these cases are from a certain class to class O. This is mainly because class O (refers to other abnormal arrhythmia except atrial fibrillation) may cover an expansive input space so that it is easier to misclassify an other class to class

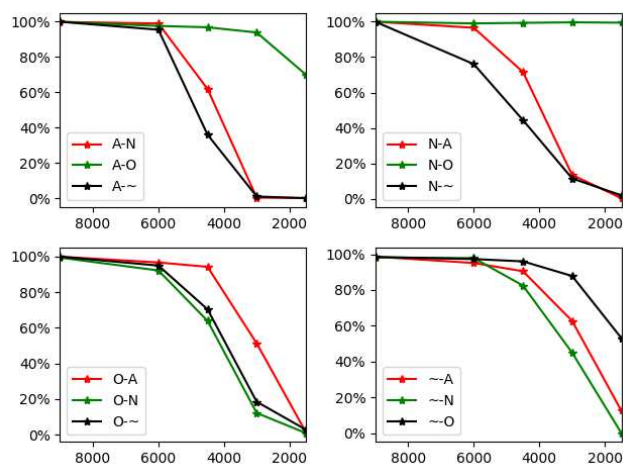


Figure 4: Success attack rates on different sized windows.

O. Besides, we find that except for class O, the success rate decrease more slowly when the target class is A. The possible reason is the inherent property of class A, *i.e.*, if a certain part of the ECG signal is regraded as atrial fibrillation, then the whole ECG segment will be classified as class A.

6 Conclusion

This paper proposes ECGadv to generate adversarial ECG examples to misguide both cloud-based and local-based arrhythmia classification systems. We identify the main issues under two different deployment models and propose effective attack schemes respectively. For attacks against the cloud model, this paper proposes a smoothness metric to encourage visual imperceptibility. Extensive human perceptual studies on both ordinary people and cardiologists validate the visual imperceptibility of the perturbations. For attacks against the local model, we model the sampling point uncertainty of the on-the-fly signals within the adversarial generation scheme.

The generated perturbations are shift-resistant to tamper on-the-fly signals with a high success rate, and universal to attacks on unseen examples. This paper reveals the blind spots of DNN-powered ECG classification systems to adversarial attacks, which facilitates future research on countermeasures.

References

- [Al Rahhal *et al.*, 2016] Mohamad M Al Rahhal, Yakoub Bazi, Haikel AlHichri, Naif Alajlan, Farid Melgani, and Ronald R Yager. Deep learning approach for active classification of electrocardiogram signals. *Information Sciences*, 345:340–354, 2016.
- [Andreotti *et al.*, 2017] Fernando Andreotti, Oliver Carr, Marco AF Pimentel, Adam Mahdi, and Maarten De Vos. Comparing feature-based classifiers and convolutional neural networks to detect arrhythmia from short segments of ecg. *Computing*, 44:1, 2017.
- [Athalye *et al.*, 2018a] Anish Athalye, Nicholas Carlini, and David Wagner. Obfuscated gradients give a false sense of security: Circumventing defenses to adversarial examples. In *International Conference on Machine Learning*, pages 274–283, 2018.
- [Athalye *et al.*, 2018b] Anish Athalye, Logan Engstrom, Andrew Ilyas, and Kevin Kwok. Synthesizing robust adversarial examples. In *International Conference on Machine Learning*, pages 284–293, 2018.
- [Awni Y *et al.*, 2019] Hannun Awni Y, Rajpurkar Pranavm, Haghpanahi Masoumeh, Tison Geoffrey H, Bourn Codie, Turakhia Mintu P, and Ng Andrew Y. Cardiologist-level arrhythmia detection and classification in ambulatory electrocardiograms using a deep neural network. *Nature Medicine*, pages volume 25, 65–69, 2019.
- [Brown *et al.*, 2017] Tom B Brown, Dandelion Mané, Aurko Roy, Martín Abadi, and Justin Gilmer. Adversarial patch. *arXiv preprint arXiv:1712.09665*, 2017.
- [Carlini and Wagner, 2017] Nicholas Carlini and David Wagner. Towards evaluating the robustness of neural networks. In *2017 IEEE Symposium on Security and Privacy (SP)*, pages 39–57. IEEE, 2017.
- [Chen *et al.*, 2018] Shang-Tse Chen, Cory Cornelius, Jason Martin, and Duen Horng Chau. Robust physical adversarial attack on faster r-cnn object detector. *arXiv preprint arXiv:1804.05810*, 2018.
- [Clifford *et al.*, 2017] Gari D Clifford, Chengyu Liu, Benjamin Moody, Li-wei H Lehman, Ikaro Silva, Qiao Li, AE Johnson, and Roger G Mark. Af classification from a short single lead ecg recording: The physionet computing in cardiology challenge 2017. *Proceedings of Computing in Cardiology*, 44:1, 2017.
- [Cuturi and Blondel, 2017] Marco Cuturi and Mathieu Blondel. Soft-dtw: a differentiable loss function for time-series. In *Proceedings of the 34th International Conference on Machine Learning-Volume 70*, pages 894–903. JMLR. org, 2017.
- [Eichmann and Zraggen, 2015] Philipp Eichmann and Emanuel Zraggen. Evaluating subjective accuracy in time series pattern-matching using human-annotated rankings. In *Proceedings of the 20th International Conference on Intelligent User Interfaces*, pages 28–37. ACM, 2015.
- [Gogolou *et al.*, 2018] Anna Gogolou, Theophanis Tsandilas, Themis Palpanas, and Anastasia Bezerianos. Comparing similarity perception in time series visualizations. *IEEE transactions on visualization and computer graphics*, 2018.
- [Goodfellow *et al.*, 2014] Ian J Goodfellow, Jonathon Shlens, and Christian Szegedy. Explaining and harnessing adversarial examples. *arXiv preprint arXiv:1412.6572*, 2014.
- [He *et al.*, 2016] Kaiming He, Xiangyu Zhang, Shaoqing Ren, and Jian Sun. Deep residual learning for image recognition. In *Proceedings of the IEEE conference on computer vision and pattern recognition*, pages 770–778, 2016.
- [IEEE-Spectrum, 2018] IEEE-Spectrum. Artificial intelligence is challenging doctors. <https://spectrum.ieee.org/static/ai-vs-doctors>, 2018.
- [Jambukia *et al.*, 2015] Shweta H Jambukia, Vipul K Dabhi, and Harshadkumar B Prajapati. Classification of ecg signals using machine learning techniques: A survey. In *Computer Engineering and Applications (ICACEA), 2015 International Conference on Advances in*, pages 714–721. IEEE, 2015.
- [Kingma and Ba, 2014] Diederik P Kingma and Jimmy Ba. Adam: A method for stochastic optimization. *arXiv preprint arXiv:1412.6980*, 2014.
- [Kiranyaz *et al.*, 2016] Serkan Kiranyaz, Turker Ince, and Moncef Gabbouj. Real-time patient-specific ecg classification by 1-d convolutional neural networks. *IEEE Transactions on Biomedical Engineering*, 63(3):664–675, 2016.
- [Kune *et al.*, 2013] Denis Foo Kune, John Backes, Shane S Clark, Daniel Kramer, Matthew Reynolds, Kevin Fu, Yongdae Kim, and Wenyuan Xu. Ghost talk: Mitigating emi signal injection attacks against analog sensors. In *Security and Privacy (SP), 2013 IEEE Symposium on*, pages 145–159. IEEE, 2013.
- [Kurakin *et al.*, 2018] Alexey Kurakin, Ian J Goodfellow, and Samy Bengio. Adversarial examples in the physical world. In *Artificial Intelligence Safety and Security*, pages 99–112. Chapman and Hall/CRC, 2018.
- [Liu *et al.*, 2016] Yanpei Liu, Xinyun Chen, Chang Liu, and Dawn Song. Delving into transferable adversarial examples and black-box attacks. *arXiv preprint arXiv:1611.02770*, 2016.
- [Moosavi-Dezfooli *et al.*, 2016] Seyed-Mohsen Moosavi-Dezfooli, Alhussein Fawzi, and Pascal Frossard. Deepfool: a simple and accurate method to fool deep neural networks. In *Proceedings of the IEEE Conference on Computer Vision and Pattern Recognition*, pages 2574–2582, 2016.
- [Moosavi-Dezfooli *et al.*, 2017] Seyed-Mohsen Moosavi-Dezfooli, Alhussein Fawzi, Omar Fawzi, and Pascal Frossard. Universal adversarial perturbations. In *Proceedings of the IEEE Conference on Computer Vision and Pattern Recognition*, pages 1765–1773, 2017.
- [Papernot *et al.*, 2016] Nicolas Papernot, Patrick McDaniel, and Ian Goodfellow. Transferability in machine learning: from phenomena to black-box attacks using adversarial samples. *arXiv preprint arXiv:1605.07277*, 2016.
- [Papernot *et al.*, 2018] Nicolas Papernot, Fartash Faghri, Nicholas Carlini, Ian Goodfellow, Reuben Feinman, Alexey Kurakin, Cihang Xie, Yash Sharma, Tom Brown, Aurko Roy, Alexander Matyasko, Wahid Behzadan, Karen Hambardzumyan, Zhishuai Zhang, Yi-Lin Juang, Zhi Li, Ryan Sheatsley, Abhibhav Garg, Jonathan Uesato, Willi Gierke, Yinpeng Dong, David Berthelot, Paul Hendricks, Jonas Rauber, and Rujun Long. Technical report on the cleverhans v2.1.0 adversarial examples library. *arXiv preprint arXiv:1610.00768*, 2018.
- [Rajpurkar *et al.*, 2017] Pranav Rajpurkar, Awni Y Hannun, Masoumeh Haghpanahi, Codie Bourn, and Andrew Y Ng. Cardiologist-level arrhythmia detection with convolutional neural networks. *arXiv preprint arXiv:1707.01836*, 2017.
- [Szegedy *et al.*, 2013] Christian Szegedy, Wojciech Zaremba, Ilya Sutskever, Joan Bruna, Dumitru Erhan, Ian Goodfellow, and Rob Fergus. Intriguing properties of neural networks. *arXiv preprint arXiv:1312.6199*, 2013.
- [World Health Organization, 2018] World Health Organization. Cardiovascular disease is the leading global killer. https://www.who.int/cardiovascular_diseases/en/, 2018.